

Temperature Dependent Sign Reversal of the Surface Contraction of Ag(111)

P. Statoris, H. C. Lu, and T. Gustafsson

*Department of Physics and Astronomy, and Laboratory for Surface Modification, Rutgers-The State University of New Jersey,
P.O. Box 849 Piscataway, New Jersey 08855-0849*

(Received 30 December 1993)

We have studied the structure of the Ag(111) surface as a function of temperature using medium energy ion scattering. We find that the first interlayer spacing is contracted at temperatures below 670 K, but increases at higher temperatures in a nonlinear fashion and is expanded some 10% 80 K below the melting point. As the surface vibration amplitudes increase significantly at the same time, we attribute this sign reversal to enhanced anharmonic effects at the surface.

PACS numbers: 68.35.Ja, 65.70.+y, 79.20.Rf

It is well established that the first interlayer separation on most metal surfaces is contracted at room temperature, with only a handful of exceptions discovered so far. In the harmonic approximation, both the surface and bulk lattice constants are temperature independent, while anharmonicity implies that these parameters will change with temperature. Because of the lower symmetry at the surface, the anharmonicity in the surface is expected to be larger than in the bulk. One would therefore expect the surface interlayer separation to increase with temperature faster than in the bulk so that a surface contraction could be turned into an expansion at high enough temperatures. This was originally predicted by Allen and de Wette [1] for noble gas crystals. Dobrzynski and Maradudin later did detailed calculations for a metal surface [Fe(001)] [2]. Experimentally, it is known that the thermal expansion coefficient is enhanced at the surface [3,4], in agreement with theoretical work [1,2,5,6]. The temperature dependence of the interlayer spacings has been studied in some cases [7-9], but a sign reversal of the first layer spacing has not yet been observed. Knowledge of the atom displacements at high temperatures can assist in the development and assessment of microscopic theories that describe the behavior of surfaces in the anharmonic regime.

In the present Letter we present medium energy ion scattering (MEIS) data for the temperature dependence of the first three surface interlayer separations (d_{12} , d_{23} , and d_{34}) and vibrational amplitudes of Ag(111). We show that at room temperature d_{12} is, as expected, contracted, but expands above 670 K in a nonlinear fashion, so that at 1150 K (80 K below the melting point), the surface is expanded by 10%. This is closely paralleled by a significant increase in the ratio of surface to bulk rms vibrational amplitudes, a ratio which is constant below 670 K. We attribute the sign reversal to enhanced anharmonic effects at the surface. Other indications of surface enhanced anharmonic effects have been observed with other techniques [10,11].

The sample was a Ag(111) disk 2 mm thick and 15 mm in diameter. Auger spectra using a double pass cylindrical mirror analyzer as well as MEIS spectra taken

after prolonged anneals showed no evidence of impurities segregating to the surface. The sample was radiatively heated by a tungsten filament. Data were taken between 300 and 1150 K. At high temperatures a calibrated optical pyrometer (accuracy $\pm 0.5\%$) was used for temperature measurements, while at temperatures lower than 870 K a Chromel-Alumel thermocouple was used. The temperature gradient over the sample surface was a few percent, while the temperature variation of the sample during measurements was less than 5 K.

MEIS is a well established quantitative high resolution technique for the study of surface structure [12]. A well collimated ion beam (97.5 keV protons in our case) is incident along a high symmetry (*channeling*) direction. The backscattered proton flux is measured as a function of energy and angle. As the scattering cross section is known, we can measure in absolute units (atoms per unit cell) the amount of material visible to the beam. The incident ion beam current is measured by intercepting a known fraction of the beam before it reaches the sample [13], while the ion energy analyzer allows the simultaneous collection of ions within a 1.8 keV energy window (at 100 keV) and a 22° angular range. The energy resolution is 150 eV at 100 keV [14]. For a rigid, perfect lattice only the first atom of each row of atoms will be visible to the ion beam. Thermal vibrations and/or relaxations will allow some ions to penetrate deeper in the crystal (Fig. 1) and backscatter off atoms in the second, third, etc., layers. The higher the vibrational amplitudes, the deeper the ions can penetrate in this way, so as the temperature increases, a significant increase in the yield occurs. This increase is a measure of the vibrational amplitudes perpendicular to the beam direction. Ions that backscatter from deeper layers cannot reach the detector if they propagate in the directions of the surface atoms. The scattered yield will therefore be reduced along these directions, resulting in a *blocking* dip in the angle dependent scattering yield (Fig. 1). The positions of the blocking dips contain information about the relative positions of the atoms within a crystal [12].

All the data were taken within the [110] scattering plane in three different scattering geometries. To quanti-

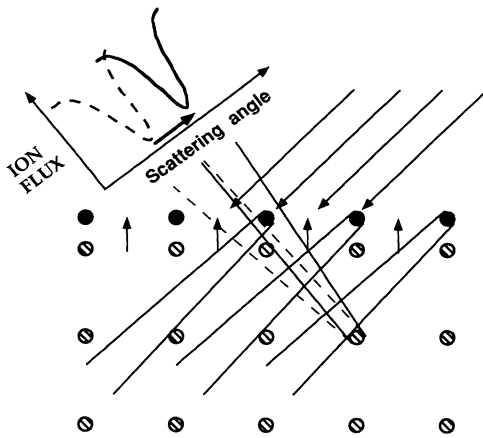


FIG. 1. Schematic figure illustrating the principle of channeling and blocking (atom sizes and relaxations exaggerated). An outwards relaxation of the surface atoms results in increased visibility of deeper layers and a shift of the blocking dip to higher scattering angles.

fy our data we perform Monte Carlo simulations of the scattering from trial structures [15]. The bulk vibrational amplitudes as well as the nearest neighbor correlation coefficients used in the simulations were determined using the Debye model. The atomic displacements due to thermal motion were taken to follow a Gaussian distribution, which is believed to be a reasonable approximation [8]. By optimizing the structural parameters in the model and comparing to the data, we arrive at the best structure. Figure 2 contains the data as well as the results of the best fit simulations for ions incident along the [110] direction. The structural parameters varied were the first three interlayer separations and the corresponding vibrational amplitudes. We allowed the vibrational amplitudes normal to the surface to vary independent of the in plane amplitudes. As the number of parameters that enter the simulations is increased (because more layers contribute to backscattering) it is possible to find more than one parameter set that provides a good fit to the data in any one geometry. The fact that we have data in different scattering geometries provides us with more stringent restrictions on the parameters.

All our simulations were performed assuming a flat, crystalline, unreconstructed, solid surface and the same atom density in all layers, assumptions which are justified by our experimental observations. Surface premelting and vacancy formation is not expected [16] to be important for a close packed surface so far below the melting point [17,18]. Our data fully support this, as the backscattering yield increases much more slowly than when premelting occurs [17,19-21]. Also, premelting is accompanied by exceptionally high vibrational amplitudes [21], *not* observed in our case. Our layer resolved blocking data show significant second-first layer blocking at all temperatures, also inconsistent with the existence of a

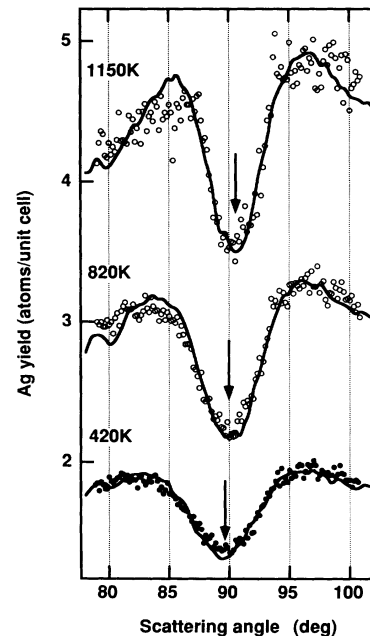


FIG. 2. Angular spectra taken at 420, 820, and 1150 K, showing the shift of the blocking dip with temperature. The solid lines are the results of the best fit simulations. The ion energy was 97.5 keV; the ions were incident in the [110] direction and collected around the [001] direction.

quasiliquid layer. A high temperature surface reconstruction like the one observed for Au(111) and Pt(111) [22-25] would give blocking spectra very different from those we observe.

The blocking dip in Fig. 2 corresponds to the [001] bulk direction (90° scattering angle). At room temperature, the surface blocking dip is shifted slightly towards lower scattering angles, corresponding to a small surface contraction. As the temperature increases, three changes occur in the spectra: The yield increases, the blocking dip shifts well past 90° (meaning that the surface goes from being contracted to being expanded), and the full width at half maximum (FWHM) of the blocking dips is reduced. The increase in the yield and the reduction of the FWHM are both indications that the vibrational amplitudes increase (deeper layers are sampled and blocking is less efficient at the same time) [19]. It is important to realize that the changes in the blocking dip position actually reflect changes in the difference between surface and bulk interplanar separations *over and above* the (smooth) increase in the bulk lattice spacing with temperature. The shift of the blocking dip position therefore indicates a nonuniform expansion coefficient perpendicular to the surface.

A plot of the temperature variation of the first three interplanar separations, as measured relative to the bulk values, is shown in Fig. 3. The surface shows a small ($\Delta d_{12}/d_{\text{bulk}} = -2.5\%$) contraction of the first layer spacing at room temperature, with an even smaller expansion

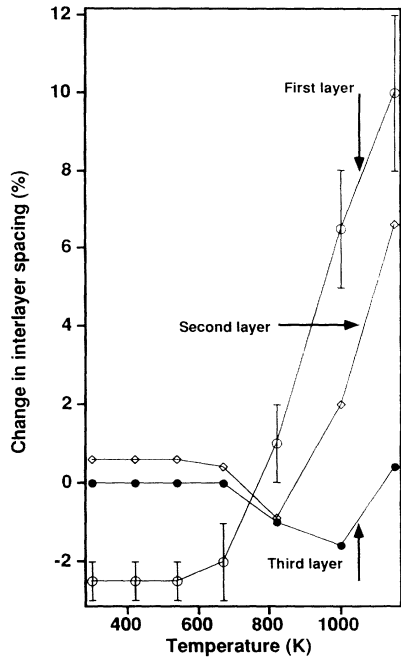


FIG. 3. Relative change in the surface to bulk interlayer spacings with temperature. Data are shown for the first three layer spacings. For clarity only the error margin in d_{12} is shown.

of d_{23} (+0.6%). (We are not at these temperatures very sensitive to changes in d_{34} from the bulk value.) There are no detectable changes in these values at temperatures below 670 K. Above 670 K a dramatic increase in the first interlayer spacing occurs, so that around 750 K $\Delta d_{12}/d_{\text{bulk}}$ crosses zero and increases to +10% at 1150 K while d_{23}/d_{bulk} increases from +0.6% at 300 K to +5.5% at 1150 K (Fig. 3). The error bars shown in Fig. 3 are determined using a goodness-of-fit test (R factor) that compares the output of our Monte Carlo scattering simulations with the data. The R -factor analysis is done for different sets of vibrational amplitudes with the constraint that the obtained yield at the shoulders of the blocking dips matches the experimental values within 3%. When this constraint is met the results in Fig. 3 are obtained. Further analysis of the data at 820 and 1000 K shows that the best results for 820 K are obtained when $d_{12} + d_{23} = 4.77 \pm 0.04 \text{ \AA}$ [$2.38 < d_{12} < 2.46 \text{ (\AA)}$] and for 1000 K when $d_{12} + d_{23} = 4.97 \pm 0.06 \text{ \AA}$ [$2.49 < d_{12} < 2.61 \text{ (\AA)}$]. The bulk interlayer spacings are 2.388 \AA at 820 K and 2.397 \AA at 1000 K. The thermal expansion coefficients can be estimated from the slope of the individual lines in Fig. 3. Since the slope is strongly temperature and layer dependent the surface thermal expansion coefficient will exhibit the same behavior. At 1000 K the first layer expansion coefficient is found to be 10 times the bulk value. At temperatures higher than 700 K the visibility of the third and fourth layers combined becomes comparable to that of the second layer. As a result the

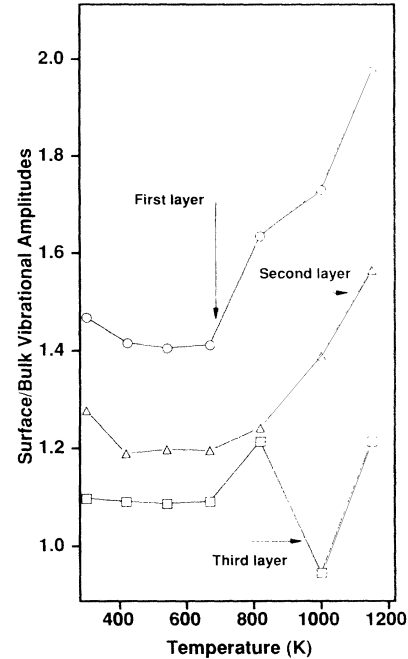


FIG. 4. rms surface vibrational amplitudes as a function of temperature. The amplitudes are normalized to the bulk values at the same temperature.

blocking dip shape depends on the combination of both d_{23} and d_{34} . We find that before the second and third interlayer spacings start to expand ($d_{23} + d_{34}$) goes through a shallow minimum. As thermal expansion is an anharmonic effect, our observations can be attributed directly to enhanced surface anharmonicity.

Concurrently with the lattice expansion an increase of the vibrational amplitudes is observed. Figure 4 shows the individual layer vibrational amplitudes normalized to the bulk value at the same temperature. Below 670 K, $\langle u_1^2 \rangle$ is $\approx 1.45 \times \langle u_b^2 \rangle$, where $\langle u_b^2 \rangle$ is the rms bulk vibrational amplitude and $\langle u_1^2 \rangle$ the rms first layer vibrational amplitude. This vibrational enhancement is rather small, implying that there is no major softening of the force constants for Ag(111) at these temperatures, in agreement with total energy calculations [26]. Above 670 K the first layer vibrational amplitude increases much more rapidly than the bulk value, so that at 1150 K the surface vibration amplitude is twice that of the bulk. While this is still far below values associated with surface melting, it is a significantly larger enhancement than that usually encountered on surfaces. There is a smaller relative enhancement of the second layer vibrational amplitude, while no significance can be attached to the small deviation from the monotonic behavior in the third layer vibrations. The simultaneous changes in the vibrational behavior and the structural parameters indicate that indeed the lattice expansion observed is related to anharmonic effects that grow stronger as the temperature rises.

Additional evidence for the existence of enhanced anharmonic effects on Ag(111) comes from a study of the Debye-Waller factor in low energy electron diffraction, where it was found that multiphonon scattering contributions to the peak intensity start appearing around 530 K and become the dominant contribution after 750 K [27]. This is the same temperature range where we observed the onset of the surface expansion.

In summary, using MEIS we have observed for the first time a sign change in the surface relaxation of Ag(111), accompanied by a rapid increase in the surface vibrational amplitudes. We attribute our results to the presence of enhanced anharmonicity at the surface.

We would like to thank Donna Saulys and Eric Garfunkel for lending us the Ag(111) crystal and Alfons Moelenbroek for information on the VEGAS simulation package, developed at the FOM Institute in Amsterdam, which was used in the simulations. This research was supported by NSF-DMR-9019868.

-
- [1] R. E. Allen and F. W. de Wette, *Phys. Rev.* **179**, 873 (1969).
- [2] L. Dobrzynski and A. A. Maradudin, *Phys. Rev. B* **7**, 1207 (1973).
- [3] A. Ignatiev and T. N. Rhodin, *Surf. Sci.* **78**, 598 (1973).
- [4] H. Zimmermann, M. Nold, U. Romahn, H. Göbel, P. von Blanckenhagen, and W. Schommers, *Surf. Sci.* **287/288**, 876 (1993).
- [5] V. E. Kenner and R. E. Allen, *Phys. Rev. B* **8**, 2916 (1973).
- [6] S. K. Ma, F. W. de Wette, and G. P. Alldredge, *Surf. Sci.* **78**, 598 (1978).
- [7] H. Göbel and P. von Blanckenhagen, *Phys. Rev. B* **47**, 2378 (1993).
- [8] J. W. M. Frenken, F. Huusen, and J. F. van der Veen, *Phys. Rev. Lett.* **58**, 401 (1987).
- [9] U. Romahn, H. Göbel, W. Schommers, and P. von Blanckenhagen, *Mod. Phys. Lett. B* **5**, 1873 (1991).
- [10] A. P. Baddorf and E. W. Plummer, *Phys. Rev. Lett.* **66**, 2770 (1991).
- [11] Y. Cao and E. Conrad, *Phys. Rev. Lett.* **64**, 447 (1990).
- [12] J. F. van der Veen, *Surf. Sci. Rep.* **5**, 203 (1985).
- [13] H. C. Lu and T. Gustafsson (unpublished).
- [14] R. M. Tromp, M. Copel, M. C. Reuter, M. H. von Hoegen, J. Speidell, and R. Koudijs, *Rev. Sci. Instrum.* **62**, 2679 (1991).
- [15] J. W. M. Frenken, R. M. Tromp, and J. F. van der Veen, *Nucl. Instrum. Methods Phys. Res., Sect. B* **17**, 334 (1986).
- [16] H. Häkkinen and M. Manninen, *Phys. Rev. B* **46**, 1725 (1992).
- [17] A. W. Denier van der Gon, R. J. Smith, J. M. Gay, D. J. O'Connor, and J. F. van der Veen, *Surf. Sci.* **227**, 143 (1990).
- [18] B. Pluis, A. W. D. van der Gon, J. W. M. Frenken, and J. F. v. d. Veen, *Phys. Rev. Lett.* **59**, 2678 (1987).
- [19] A. Hoss, U. Romahn, M. Nold, and P. von Blanckenhagen, *Phys. Rev. B* **45**, 8714 (1992).
- [20] A. Hoss, U. Romahn, M. Nold, P. von Blanckenhagen, and O. Meyer, *Europhys. Lett.* **20**, 125 (1992).
- [21] J. W. M. Frenken and J. F. van der Veen, *Phys. Rev. Lett.* **54**, 134 (1985).
- [22] J. V. Barth, H. Brune, G. Ertl, and R. J. Behm, *Phys. Rev. B* **42**, 9307 (1990).
- [23] A. R. Sandy, S. G. J. Mochrie, D. M. Zehner, K. G. Huang, and D. Gibbs, *Phys. Rev. B* **43**, 4667 (1991).
- [24] A. R. Sandy, S. G. J. Mochrie, D. M. Zehner, G. Grübel, K. G. Huang, and D. Gibbs, *Phys. Rev. Lett.* **68**, 2192 (1992).
- [25] A. R. Sandy, S. G. J. Mochrie, D. M. Zehner, G. Grübel, K. G. Huang, and D. Gibbs, *Surf. Sci.* **287/288**, 321 (1993).
- [26] Y. Chen, S. Y. Tong, K. P. Bohnen, T. Rodach, and K. M. Ho, *Phys. Rev. Lett.* **70**, 603 (1993).
- [27] R. L. Dennis and M. B. Webb, *J. Vac. Sci. Technol.* **10**, 192 (1973).